

J. Environ. Treat. Tech.

ISSN: 2309-1185

Journal weblink: http://www.jett.dormaj.com



Preparation of Zn_xFe_{3-x}O₄@chitosan Nanoparticles as an Adsorbent for Methyl Orange and Phenol

Mina Gholami^{1,2}, Alireza Zare-Hoseinabadi³, Mohammad Mohammadi³, Saeed Taghizadeh⁴, Abbas Behzad Behbahani^{1,2}, Ali Mohammad Amani^{3*}, Rita Arab Solghar^{1,2*}

- ¹ Diagnostic Laboratory Sciences and Technology Research Center, School of Paramedical Sciences, Shiraz University of Medical Sciences, Shiraz, Iran.
- ² Department of Medical Laboratory sciences, School of Paramedical Sciences, Shiraz University of Medical Sciences, Shiraz, Iran
 ³ Department of Medical Nanotechnology, School of Advanced Medical Sciences and Technologies, Shiraz University of Medical Sciences, Shiraz, Iran
- ⁴ Department of Medical Biotechnology, School of Advanced Medical Sciences and Technologies, Shiraz University of Medical Sciences, Shiraz, Iran

Abstract

We have propounded an easy preparation process for the synthesis of chitosan-covered $ZnxFe_3-xO_4$ nanoparticles by the application of $FeCl_2.4H_2O$, $FeCl_3.6H_2O$, and Zinc Acetate. The synthesized nanoparticles, which went through various analysis methods, including transmission electron microscopy (TEM), scanning electron microscope (SEM), Energy-dispersive X-ray spectroscopy (EDS), X-ray diffraction (XRD), vibrating-sample magnetometer (VSM), and Fourier transform infrared (FT-IR) spectroscopy, were later on exploited as adsorbent for phenol and Mo contaminations. Trapped within a matrix of chitosan, the synthesized $ZnxFe_3-xO_4$ nanoparticles had a size of less than 30nm. The EDS and FTIR analysis methods demonstrated the presence of Zn element inside the structure and the NH $_2$ group on nanoparticles' surface, respectively. The coated nanoparticles had a magnetic saturation of 55 emu/g. Accordingly, the results showed that the synthesized nanoparticles had a very high capacity phenol and methyl adsorption.

Keyword: Ferrite Magnetite, ZnFe₂O₄, NH₂ Magnetic Nanobeads, chitosan

1 Introduction

Nowadays, with the increasing spread of textile, leather, cosmetics, and pharmaceuticals, concerns about pollutants in the said industries, which are mainly colored and phenolic pollutants, are increasing (1). Dye contaminations cause minor changes in the color of aquatic environments and disrupt aquatic bio-processes (2). Methyl Orange (MO) is one of the most important colorant contaminations of the said industries due to its complex chemical structure, low biodegradability, and the Azo group presented in the structure (3).

A number of methods can be used for eliminating these sorts of environmental pollutions, including biological treatments, bioseparation, separation through membranes (4), photolysis (5), precipitation (1), oxidation (6), and adsorption (2). Due to its high efficiency, simplicity, low cost, and repeatability, the adsorption method has been widely recommended (2). Possessing unique magnetic properties and high reactivity, iron magnetite nanoparticles are of considerable importance amongst different adsorbents (2, 7). Separation of the iron magnetite with an external magnetic force, facilitates the adsorbing process, reduces the

costs, and increases the efficiency (2).

Iron magnetite nanoparticles' crystal structure follow a spinel pattern composed of Fe²⁺ and Fe³⁺ ions accompanied by oxygen. Magnetic and biological properties of Fe₃O₄ can be tailored through manipulating its stoichiometry and crystal structure (8). One of the most important factors that affects the intensity and stability of the magnetic properties of iron magnetite nanoparticles is the substitution of other metal cations within the structure (9). Doping metals such as Zn, Co, Pt, and Mn to the magnetite, leads to changes in its stoichiometry and magnetization. Recent studies have shown that slight amounts of Zinc substitution could increase the saturation magnetization (7, 10-12). In this case, using zinc ferrite magnetite leads to facile control of magnetic properties compared with Fe₃O₄ (13).

Ferrite magnetite structures can be actually functionalized with polymeric coatings so as to enhance its level of responsiveness (14). Coating with polymers, in addition to increasing the number of active agent groups on the surface of the nanoparticles, can practically generate a matrix which is sensitive to pH, temperature, light, etc. Chitosan, for instance, having OH and NH2 groups on its

Corresponding Author: Ali Mohammad Amani, Department of Medical Nanotechnology, School of Advanced Medical Sciences and Technologies, Shiraz University of Medical Sciences, Shiraz, Iran; E-mails: amani_a@sums.ac.ir.

surface, shows desirable efficiency in the removal of azo dyes (14, 15). Chitosan is a natural polysaccharide made by treating the chitin shells of shrimp and other crustaceans through N-deacetylation. The solubility and molecular weight of chitosan is largely defined by the source of the chitin and the conditions surrounding its deacetylation (16).

In the present study, a simple and single-step synthesis method was used to produce chitosan coated nanoparticles. Afterwards, the synthesized nanocomposites were characterized by transmission electron microscopy (TEM), scanning electron microscope (SEM), Energy-dispersive X-ray spectroscopy (EDS), X-ray diffraction (XRD), vibrating-sample magnetometer (VSM), and Fourier transform infrared (FT-IR) spectroscopy. Ultimately, they were exploited for Mo and Phenol removal from the aqueous environments.

2 Materials and methods

2.1 Chemicals and Reagents

Zinc acetate $(Zn(CH_3CO_2)_2 \cdot 2H_2O)$, iron(II) chloride tetrahydrate (FeCl₂·4H₂O), iron(III) chloride hexahydrate (FeCl₃·6H₂O), acetic acid, sodium hydroxide (NaOH), and ammonium hydroxide (NH₄OH, 25 wt %) were purchased from Merck Chemicals (Darmstadt, Hessen, Germany). Methyl Orange ($C_{14}H_{14}N_3NaO_3S$), phenol (C_6H_6O), and Chitosan (reagent grade, N85% deacetylation, low molecular weight of 50,000–190,000 g/mol) were purchased from the Sigma Chemical Co., USA.

2.2 Synthesis of ZnxFe3-xO4-chitosan Core-Shell

Co-precipitation method has been employed to turn ZnxFe₃-xO₄ nanoparticles into synthesis of sorts. In the case under our own discussion, 5.4 grams of FeCl₃.6H₂O in addition to 1.99g FeCl₂.4H₂O and 0.8g Zn(CH₃CO₂)₂ .2H₂O were actually solved into the liquid amount of 50 ml volume of deionized water. This process was, of course, enacted with its later being strongly shaken. What was in mind, was in fact bringing up the level of pH up to 10. It was for this reason that 25% wt of NH₄OH was also brought into the process. The ensuing reaction went on to take 2h with the condition that the ambient atmosphere gas was N2 while the surrounding temperature was kept at 80 °C (17). Henceforward, the nanoparticles that were this way synthesized cold then be washed with deionized water. Such washing was continued till coming to a pH of neutrality. The next step was that preparation was made for a solution of 50ml acetic acid and 0.12 g chitosan. This preparation had also two dry grams of Zn_XFe₃-_XO₄ synthesized nanoparticles as an addition. For purposes of coming to even, homogenous dispersal of the said Zn_xFe_{3-x}O₄ inside the chitosan solution, stirring vehemently was imposed for half an hour. In the end, by the means of adding 50ml NaOH onto the mixture, Zn_XFe_{3-X}O₄ nanoparticles were finally able to be coated with chitosan. It is to be noted that these particles could later be well washed with deionized water to be stored at the temperature of 4°C to become immobilized (18).

2.3 Characterization

The visual appearance and the morphology of the Zn_XFe_{3-X}O₄@chitosan were investigated by scanning electron microscopy (SEM), using ZEISS SIGMA VP field

emission scanning electron microscope (FE-SEM) w/EDX&EBSD and by transmission electron microscopy (TEM), using a ZEISS 10A conventional TEM model Carl Zeiss-. EM10C-100 KV(Germany). FTIR spectra were carried out employing a Fourier transform infrared spectrophotometer (Nicolet IS10, Thermo Scientific, USA). The scanning range of the scanning wavenumbers was in the range 400–4000 cm-1, using KBr pellets. The crystalline structure characterized by Powder X-ray diffraction was conducted with a PANalytical X'Pert Pro (UK) instrument. A vibrating sample (VSM, LBKFB, Meghnatis Daghigh. Kavir Co) magnetometer was used to obtain magnetization curves.

2.4 Experiment on adsorption

The adsorption experiments have actually been conducted at the temperature of 25 °C and pH = 4 through the utilization of a thermostated shaker with a rate of 200 rpm. Both of the pollutant materials; that is to say, phenol and MO, had some concentrations in the range of 100 mgl. Batch-mode adsorption studies were carried out by adding 100.0 mg adsorbent and 100.0 mL solution of contamination (2, 15). After dye adsorption, ZnxFe_{3-x}O₄@chitosan were quickly separated from the sample solution in various time intervals (15 min, 30 min, 60 min, and 120 min) applying a magnet. The concentration monitoring could be carried out by the application of a peculiar model of UV-Vis spectrometer (model UVmini-1240 SHI-MADZU). Value guesstimation was also possible when we applied the upper ceiling of the likely wavelength; it turned out to be 270nm for phenol and 646nm for MO. The following equation was employed to calculate the adsorption efficiency of the pollutants in the treatment experiments: where Ci and Cr are the initial and residual concentrations of the pollutants in the solution, respectively

3.1 Characterization

The SEM image (Figure 1) of the synthesized $Zn_XFe_{3-}xO_4$ @chitosan nanocapsites shows that the coating of the chitosan polymers on the surface of the magnetite ferrite nanoparticles is carried out well; the coated nanoparticles are mostly in the form of complexes of chitosan and several nanoparticles next to each other. In view of the image, the size of the coated nanoparticles is mostly below 30 nanometers. The TEM image (Figure 2) can make it quite clear that the nanoparticles coated with chitosan are very well covered by them. It also illustrates fairly clearly that the presence of complexes imbricated all into each other is coated with chitosan covering. According to the TEM image, magnetite ferrite nanoparticles are inside the bedding of a chitosan polymer: thus, they provide a broad magnetic polymer structure.

We can see (in Figure 3) the FTIR absorption spectra belonging to the synthesized Zn_XFe_{3-X}O₄@chitosan. The peak inside the 560 cm⁻¹ region, emblematic of the Fe-O group, can be found within the Zn_XFe_{3-X}O₄@chitosan spectra. This actually confirms the fact that the product is comprising of magnetite (19, 20). The peaks over around 1630 cm⁻¹, attributed to the N-H group and the adsorption peak at 3416 cm⁻¹ do relate to the stretching of O-H (18).

This, in fact, proves that particles of magnetite had been successfully coated with the intended polymer.

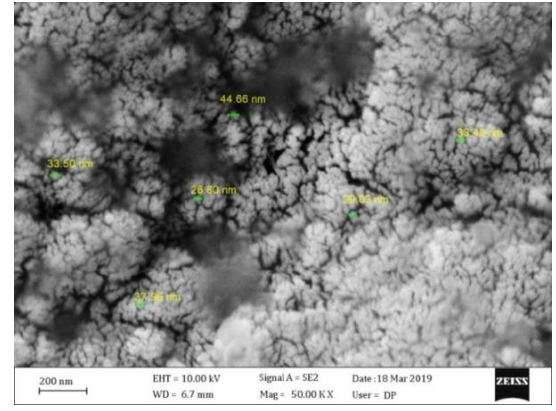


Figure 1: SEM image of Zn_XFe_{3-X}O₄ @chitosan

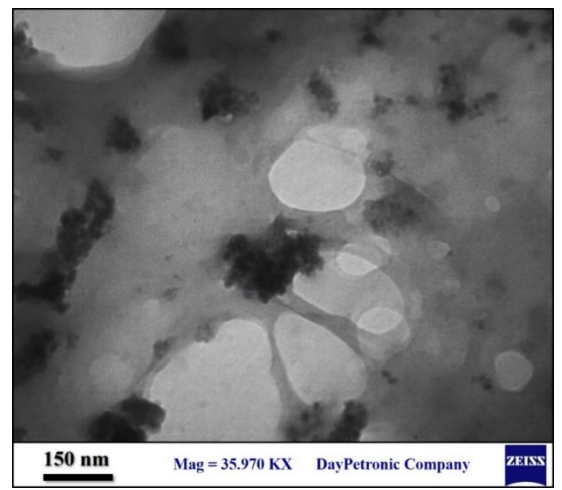


Figure 2: TEM image of Zn_XFe_{3-X}O₄ @chitosan

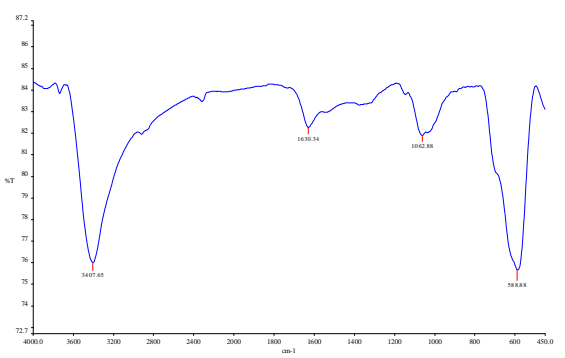


Figure 3: FTIR spectra of Zn_XFe_{3-X}O₄ @chitosan

The crystalline phase of the prepared Zn_XFe_{3-X}O₄@chitosan was evaluated by X-ray powder diffraction analysis. As shown in Figure 4, there are five peaks within the regions 220, 311, 400, 511, and 440, which represent the reverse magnetic crystalline structure (19, 21, 22). Additionally, we were not able to detect observable patterns in correspondence to Zincite (ZnO). This in itself can suggest

that zinc is present merely inside the structure of magnetite crystal (13).

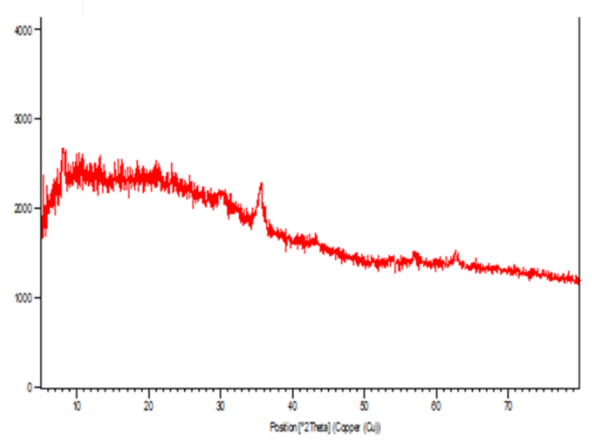


Figure 4: X-ray diffraction patterns of Zn_XFe_{3-X}O₄ @chitosan

Figure 5 brings out the weight percentage of the elements which make up the nanoparticles coated with chitosan, applying EDS analysis. The presence of significant amounts of carbon and nitrogen among the component elements, implies that chitosan has well covered the surface of the nanoparticles: the covering is complete. This graph also indicates that Zn^{2+} cation is thoroughly kept in place beside Fe^{2+} and Fe^{3+} ions.

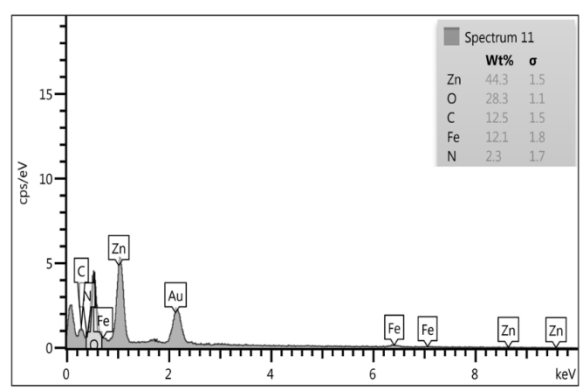


Figure 5: EDS analysis graph of Zn_XFe_{3-X}O₄ @chitosan

Curves representing $Zn_xFe_{3-x}O_4$ and $Zn_xFe_{3-x}O_4$ @chitosan magnetization at room temperature have been put forward in figure 6. High saturation magnetization (σ s) could be seen on the part of immobilized cellulose: it was around 55 emu/g. However high saturation magnetization (σ s) as for pure $Zn_xFe_{3-x}O_4$ turned out to be 70 emu/g. The results thus indicate that any chitosan coating has had its effect on the magnetism of resultant nanoparticles. This was due to the presence of diamagnetic chitosan. Still, this manner of magnetism permits for the supports to be regained rather quickly from the system of decontamination reactions through the application of an external magnetic field. This is some significant advantage in desorption/adsorption techniques.

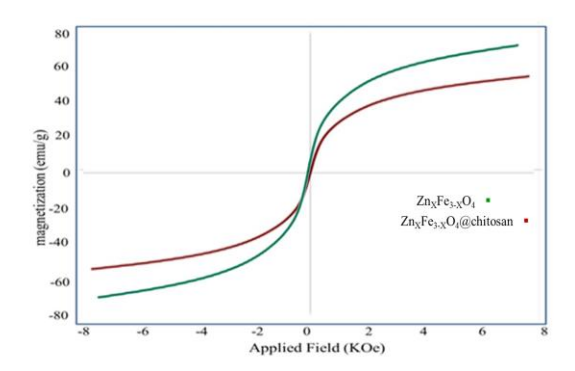


Figure 6: VSM graph of the nanoparticles coated with chitosan

3.2 Experiment on adsorption

The efficiency of synthesized $Zn_XFe_{3-X}O_4$ @chitosan in adsorbing MO and phenol is presented in Figure 7. In this case, pollutants adsorption found to be a time dependent process in the presence of $Zn_XFe_{3-X}O_4$ @chitosan. Exposing MO and phenol to $Zn_XFe_{3-X}O_4$ @chitosan for 120 min, the adsorption efficiency was calculated to be 88% and 83%, respectively. The results indicated that $Zn_XFe_{3-X}O_4$ @chitosan nanocomposite can be employed as a suitable and powerful adsorbent for MO and phenol removal purposes.

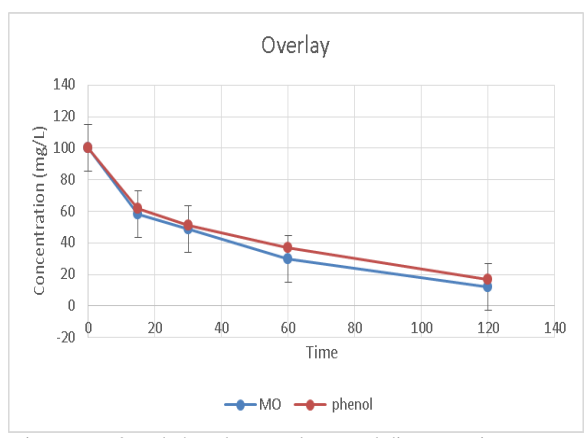


Figure 7: MO and phenol removal removal diagram using Zn_XFe_3 . $_XO_4$ @chitosan

4 Conclusion

According to the TEM image, magnetite ferrite nanoparticles are inside the bedding of a chitosan polymer: thus, they provide a broad magnetic polymer structure. EDS analysis also indicates that Zn^{2+} cation is thoroughly kept in place beside Fe^{2+} and Fe^{3+} ions. Consequently, the results showed that the synthesized nanoparticles were hugely capable of phenol and methyl adsorption.

References

 Zhu M-X, Lee L, Wang H-H, Wang Z. Removal of an anionic dye by adsorption/precipitation processes using alkaline white mud. Journal of Hazardous Materials. 2007;149(3):735-41.

- Istratie R, Stoia M, Păcurariu C, Locovei C. Single and simultaneous adsorption of methyl orange and phenol onto magnetic iron oxide/carbon nanocomposites. Arabian Journal of Chemistry. 2016.
- Lima-Tenório MK, Oliveira LA, Guilherme MR, Tenório-Neto ET, Silva MF, Fernandes DM, et al. Tuning the magnetic properties of ferrite nanoparticles by Zn and Co doping. Materials Letters. 2017;195:151-
- Alventosa-deLara E, Barredo-Damas S, Alcaina-Miranda M, Iborra-Clar M. Ultrafiltration technology with a ceramic membrane for reactive dye removal: optimization of membrane performance. Journal of Hazardous materials. 2012;209:492-500.
- 5. Guo Z, Ma R, Li G. Degradation of phenol by nanomaterial TiO2 in wastewater. Chemical engineering journal. 2006;119(1):55-9.
- Duan F, Li Y, Cao H, Wang Y, Crittenden JC, Zhang Y. Activated carbon electrodes: Electrochemical oxidation coupled with desalination for wastewater treatment. Chemosphere. 2015;125;205-11.
- Usman M, Byrne J, Chaudhary A, Orsetti S, Hanna K, Ruby C, et al. Magnetite and green rust: synthesis, properties, and environmental applications of mixedvalent iron minerals. Chemical reviews. 2018;118(7):3251-304.
- 8. Srivastava M, Alla S, Meena SS, Gupta N, Mandal R, Prasad N. Zn x Fe 3− x O 4 (0.01≤ x≤ 0.8) nanoparticles for controlled magnetic hyperthermia application. New Journal of Chemistry. 2018;42(9):7144-53.
- Hoque SM, Hossain MS, Choudhury S, Akhter S, Hyder F. Synthesis and characterization of ZnFe2O4 nanoparticles and its biomedical applications. Materials letters. 2016;162:60-3.
- Usman M, Byrne JM, Chaudhary A, Orsetti S, Hanna K, Ruby C, et al. Magnetite and Green Rust: Synthesis, Properties, and Environmental Applications of Mixed-Valent Iron Minerals. Chem Rev. 2018;118(7):3251-304
- Liu J, Bin Y, Matsuo M. Magnetic behavior of Zn-doped Fe3O4 nanoparticles estimated in terms of crystal domain size. The Journal of Physical Chemistry C. 2011;116(1):134-43.
- Moise S, Cespedes E, Soukup D, Byrne JM, El Haj AJ, Telling ND. The cellular magnetic response and biocompatibility of biogenic zinc- and cobalt-doped magnetite nanoparticles. Sci Rep. 2017;7:39922.
- Byrne JM, Coker VS, Cespedes E, Wincott PL, Vaughan DJ, Pattrick RA, et al. Biosynthesis of zinc substituted magnetite nanoparticles with enhanced magnetic properties. Advanced Functional Materials. 2014;24(17):2518-29.
- 14. Ignat M, Samoila P, Cojocaru C, Sacarescu L, Harabagiu V. Novel synthesis route for chitosan-coated zinc ferrite nanoparticles as potential sorbents for wastewater treatment. Chemical Engineering Communications. 2016;203(12):1591-9.
- Munagapati VS, Yarramuthi V, Kim D-S. Methyl orange removal from aqueous solution using goethite, chitosan beads and goethite impregnated with chitosan beads. Journal of Molecular Liquids. 2017;240:329-39.

- 16. Elieh-Ali-Komi D, Hamblin MR. Chitin and chitosan: production and application of versatile biomedical nanomaterials. International journal of advanced research. 2016;4(3):411.
- 17. Sanpo N, Wen C, Berndt CC, Wang J. Multifunctional spinel ferrite nanoparticles for biomedical application. Advanced Functional Materials. 2015:183-217.
- 18. Zang L, Qiu J, Wu X, Zhang W, Sakai E, Wei Y. Preparation of magnetic chitosan nanoparticles as support for cellulase immobilization. Industrial & engineering chemistry research. 2014;53(9):3448-54.
- 19. Kouhbanani MAJ, Beheshtkhoo N, Taghizadeh S, Amani AM, Alimardani V. One-step green synthesis and characterization of iron oxide nanoparticles using aqueous leaf extract of Teucrium polium and their catalytic application in dye degradation. Advances in Natural Sciences: Nanoscience and Nanotechnology. 2019;10(1):015007.
- 20. Lohrasbi S, Kouhbanani MAJ, Beheshtkhoo N, Ghasemi Y, Amani AM, Taghizadeh S. Green Synthesis of Iron Nanoparticles Using Plantago major Leaf Extract and Their Application as a Catalyst for the Decolorization of Azo Dye. BioNanoScience. 2019:1-6.
- 21. Samimi-Sedeh S, Saebnoori E, Talaiekhozani A, Fulazzaky MA, Roestamy M, Amani AM. Assessing the Efficiency of Sodium Ferrate Production by Solution Plasma Process. Plasma Chemistry and Plasma Processing. 2019:1-18.
- 22. Talaiekhozani A, Banisharif F, Bazrafshan M, Eskandari Z, Chaleshtari AH, Moghadam G, et al. Comparing the ZnO/Fe (VI), UV/ZnO and UV/Fe (VI) processes for removal of Reactive Blue 203 from aqueous solution. Environmental Health Engineering and Management Journal. 2019.